Journal of Applied Polymer Science

Degradability of Extruded Polyethylene/Chitosan Blends Compatibilized with Polyethylene-*Graft*-Maleic Anhydride Under Natural Weathering

Dora Evelia Rodríguez-Félix,[1] Jesús Manuel Quiroz-Castillo,[1] Heriberto Grijalva-Monteverde,[1] Teresa del Castillo-Castro,[1] Silvia Elena Burruel-Ibarra,[1] Francisco Rodríguez-Félix,[2] Tomás Madera-Santana,[3] Rafael Enrique Cabanillas,[4] Pedro Jesús Herrera-Franco[5]

[1]Departamento de Investigación en Polímeros y Materiales, Universidad de Sonora, P.C. 83000, Hermosillo Sonora, México
[2]Departamento de Investigación y Posgrado en Alimentos, Universidad de Sonora, P.C. 83000, Hermosillo Sonora, México
[3]Laboratorio de Envases, CTAOV, Centro de Investigación en Alimentos y Desarrollo A.C. P.C. 83304, Hermosillo Sonora, México
[4]Departamento de Ingeniería Química y Metalurgia, Universidad de Sonora, P.C. 83000, Hermosillo Sonora, México
[5]Centro de Investigación Científica de Yucatán, Unidad de Materiales, P.C. 97200, Mérida Yucatán, México
Correspondence to: J. M. Quiroz-Castillo (E-mail: quiroz51@hotmail.com)

ABSTRACT: The impact of chitosan on the natural weathering behavior of two blends obtained by mixing either polyethylene (PE) with chitosan or PE, chitosan and polyethylene-*graft*-maleic anhydride (PEgMA) as a compatibilizer is analyzed. In order to follow the weathering behavior of both the uncompatibilized and compatibilized systems, the blend films are exposed to outdoor conditions for 6 months. The weathering behavior of the films is monitored by mechanical tests, spectroscopic Fourier transform infrared, and morphological analyses at different weathering periods of time. The presence of chitosan in the blends accelerates significantly the degradation of the films. Apparently, PEgMA also accelerates the photo-oxidation rate of the films. This behavior appears to be related to the photo-oxidative instability of maleic anhydride, and also to the better dispersion of chitosan in the PE matrix, which is due to the interactions in the PE/chitosan interface caused by the addition of the compatibilizer. © 2014 Wiley Periodicals, Inc. J. Appl. Polym. Sci. **2014**, *131*, 41045.

KEYWORDS: mechanical properties; polyolefins; polysaccharides; properties and characterization

Received 31 January 2014; accepted 13 May 2014
DOI: 10.1002/app.41045

INTRODUCTION

Polyolefin-based polymers are the most produced and consumed synthetic polymers worldwide; the high stability of these compounds and their significant resistance to degradation has led to their accumulation in the environment.[1] This accumulation is a matter of great concern leading to long-term environment, economic, and waste management problems.[2] One promising possible alternative to solve this problem, for the case of plastic waste, is the development of polymers that are degraded by the environment in short periods of time.[3]

Natural weathering, which includes solar radiation, wind, and ambient temperature, leads to the formation of free radicals, which may combine with oxygen on the surface and form peroxides and hydroperoxides, following the known reactions of oxidative degradation.[4] Structural defects such as unsaturation, as well as carbonyl or hydroperoxide groups, may be formed in polyolefin-based polymers during polymerization and processing; these defects could enhance their degradation rate, nevertheless, they are present at very low levels.[5,6]

A wide variety of synthetic polymers absorbs solar ultraviolet (UV) radiation and undergoes photolytic, thermo-, and photo-oxidative reactions that result in the degradation of these materials.[7,8] Photo-oxidative degradation is the process of deterioration of the material by the action of light; this is considered the most important degradation mechanism of synthetic polymers during natural weathering. Normally, the near-UV radiations (290–400 nm) in the sunlight determine the lifetime of polymeric materials in outdoor applications.[4] Several reports conclude that temperature also plays an important role in degradation rate; when polymers are exposed to the same dose of radiation,[9] the degradation rate is accelerated as temperature increases.[10,11]

Polyethylene (PE) films when exposed to UV radiation lose their extensibility, mechanical integrity, and strength along with decrease in their average molecular weight.[12,13] Naturally occurring polymers, also known as biopolymers, absorb solar radiation and undergo photolytic, photo-oxidative, and thermo-oxidative reactions that result in the degradation of the material.[10]

Table I. Concentration of Each Component Used in the Preparation of PE/Chitosan Blends

	Concentration in composites			
Code	PE (wt %)	Chitosan (wt %)	PEgMA (wt %)	Glycerol (g/g chitosan)
A	100	0	0	0
B	85	15	0	2
C	80	15	5	2

The search for low-cost, environmentally friendly materials has led toward the development of different biodegradable plastics, incorporating natural polymers into commodity plastics[14–17]; this kind of polymer blends have gained much interest in past years and are becoming more and more important because of the favorable balance of properties, cost, and environmental impact.[18]

Natural polymers are hydrophilic, whereas synthetic polymers are hydrophobic in nature. The resulting blend of these two types of polymers is generally immiscible. Polymers grafted with maleic anhydride are used as compatibilizers for immiscible binary mixtures, showing good results.[19–21]

The attention of this research is focused on blends of PE and chitosan. Chitosan films have shown great potential to be used as packaging material due to their antimicrobial activity and nontoxicity. Moreover, chitosan is sensitive to various types of degradation such as oxidative, hydrolytic, thermo-, photo-, and ultrasonic degradation.[1,22–26]

In our previous work, PE/chitosan composite films with a maximum chitosan content of 20 wt % were successfully extruded using polyethylene-*graft*-maleic anhydride (PEgMA) as a compatibilizer.[27]

The objective of this study is focused on analyzing the impact of chitosan on the natural weathering behavior of two blends obtained by mixing either PE with chitosan or PE, chitosan, and PEgMA as a compatibilizer. The weathering behavior of the films was monitored by mechanical tests, spectroscopic Fourier transform infrared (FTIR), and morphological analyses at different weathering periods.

The presence of chitosan in the blends accelerates the degradation rate of the films significantly. Apparently, PEgMA also accelerates the photo-oxidation rate of the films. This behavior appears to be related to the better dispersion of chitosan in the PE matrix, due to interactions in the PE/chitosan interface caused by the addition of PEgMA.

EXPERIMENTAL

Materials

Chitosan of medium molecular weight (molecular weight of 190,000–310,000 Da, and 75–85% deacetylated), PEgMA (with 3.5% maleic anhydride), and glycerol were obtained from Sigma-Aldrich. Commercial grade low density PE (melt flow rate 2.0 g/10 min with 2.16 kg standard die at 190°C) was obtained from Qatar Petrochemical Company (QAPCO). PE was milled and chitosan was dried at 110°C for 24 h before usage, PEgMA and glycerol were used as received.

Polymer Processing and Films Preparation

The polymeric blends were prepared using our previously reported method,[27] which consisted of two stages: (1) mixing chitosan with glycerol (plasticizer) to obtain a homogeneous mass and (2) mixing plasticized chitosan with PE and PEgMA (compatibilizer). Both stages were carried out by mechanical agitation for 30 min. The blends were then extruded in an Atlas laboratory mixer-extruder, with a speed of 40 rpm. The temperatures were controlled at 130 and 140°C for the screw barrel and the flat die, respectively, except for the pure PE film; in this case, the temperatures were controlled at 115 and 125°C. Table I indicates the concentration of each component on each prepared blend.

Natural Weathering Exposure

The test site was located in the rural-urban semi-arid atmosphere of the city of Hermosillo (29° 05′ N, 110° 57′ W; 282 m.a.s.l.), 100 km off the Gulf of California in the Pacific coast.

The films were cut into specimens (geometry and dimensions in accordance to ASTM D1708) and exposed on a stationary rack fixed to the laboratory roof at the site latitude angle (35°). Samples were taken and characterized at 45, 90, 135, and 180 days during the experimental period (March–August, 2013). On-site temperature and humidity were recorded every hour by a data logger (HOBO® Onset Computer Corp.) placed on the rack and close to the samples. Location irradiance data during the experimental period were obtained from the Solar Monitoring Station in the Agriculture Department (University of Sonora). The UV irradiation (290–385 nm) was estimated using the equation proposed by Al-Aruri,[28] which is an empirical relationship between global radiation and global UV solar radiation components.

Films Characterizations

FTIR Analysis. FTIR spectroscopy of the blends, before and after weathering, was performed using a FTIR Perkin-Elmer 1600 spectrophotometer. The spectrum was scanned from 4000 to 400 cm^{-1}. An average of 32 scans was recorded. Approximately 5 mg of dry sample were directly embedded into a KBr pellet and measured in transmittance mode.

Mechanical Characterization. The mechanical properties of the composite films were measured in a tensile loading mode using a United SSTM-5KN universal testing machine equipped with a load cell of 5 kN at a cross-head speed of 10 mm min^{-1}. At least eight specimens from each film were tested, and the average values are reported in this document. The thickness of the film was measured with a Mitutoyo micrometer.

Morphological Characterization. Morphological changes were described based on images of the films. A typical specimen from each film and weathering time was selected and observed by visual inspection, documented by photography. Surface morphology of the samples was examined using a MD600E AmScope stereo microscope and a scanning electron microscope (SEM) (JEOL JSM-5410LV), equipped with an INCA system

Table II. Weather Conditions During Natural Weathering Test Starting March 1st, 2013

Period of weather tests	Estimated cumulative UV irradiation (MJ m^{-2})	Cumulative irradiation (MJ m^{-2})	Average daily irradiation (MJ m^{-2})	Average daily highest irradiance (W m^{-2})	Average daily relative humidity (%)	Average daily temperature (°C)
March 1 to April 14	54.25	1130.48	25.12	990.02	25.29	25.52
April 15 to May 29	117.24	2442.73	29.16	1058.93	23.48	29.49
May 30 to July 13	178.73	3723.81	28.43	1017.63	33.19	36.07
July 14 to August 27	230.97	4812.11	23.91	986.74	43.54	38.03

and an energy dispersive X-ray detector (Oxford Instrument), and operated at a voltage of 20 kV. For SEM analysis, the specimens were cut to an appropriate size and mounted on a copper sample holder using carbon double-sided stick tape; the specimens were coated with gold to provide conduction and prevent charging under electron bombardment. Observation of the sample was performed under high vacuum using the secondary electron detector.

RESULTS AND DISCUSSION

Natural Weathering Exposures

In the Mexican northwest semi-arid climate, temperatures follow a cycle of warming beginning in April, a peak in July, and a gradual decrease beginning with rains in August–September, until finally reaching minimum levels in December–January due to cooler northerly winds.

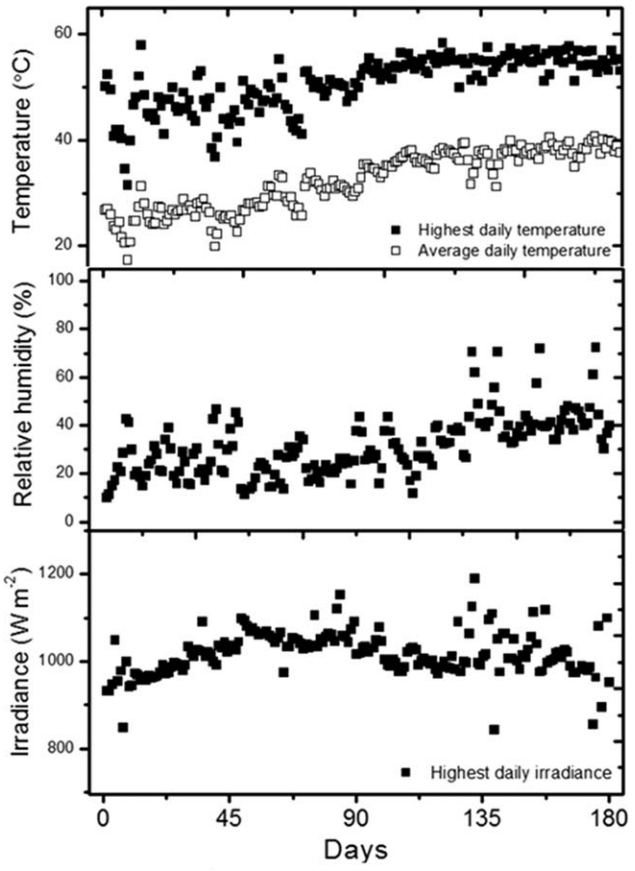

Figure 1. Daily weather conditions during natural weathering test starting March 1st, 2013.

The estimated cumulative UV irradiation values and other relevant weather conditions during the weathering test periods are reported in Table II; daily average values for temperature, relative humidity, and irradiance are reported in Figure 1.

FTIR Analysis

FTIR spectra of the prepared films are shown in Figure 2; the wavenumber range is 4000–400 cm^{-1} in Figure 2(a,c,e), and 2000–1500 cm^{-1} in Figure 2(b,d,f). Carbonyl index (CI) was calculated using the ratio of absorption bands at 1712 and 2020 cm^{-1}.[29] Figure 3 shows the change in the CI as a function of natural weathering time; the value of CI for all the specimens, before natural weathering, was zero. FTIR spectra for the PE films before weathering [Figure 2(a-1,b-1)] showed the characteristic peaks of PE: (1) hydrocarbon stretching peak around 2800–3000 cm^{-1}, (2) methylene scissoring peak at 1467 cm^{-1}, and (3) methylene rocking band at 722 cm^{-1}.[16] After 45 days of exposure, a new band appeared at 1712 cm^{-1} [Figure 2(a-2,b-2)], which indicated the presence of carbonyl groups; this was also confirmed by the CI, which was calculated and equaled 1.8 (Figure 3). The appearance of carbonyl moiety is an expected structural change caused by photodegradation. It can also be noticed that the area under this band continually increased with weathering time in a linear behavior, with CI values of 5.5, 8.9, and 11 after 90, 135, and 180 days, respectively (Figure 3). These results are consistent with several reports of PE degradation.[1,4,7,9,18,30,31]

Before weathering, FTIR spectra for the PE/chitosan films [Figure 2(c-1,e-1)] showed the characteristic bands of the individual polymers, the stretching of the OH group of chitosan appeared at 3365 cm^{-1}; bands at 2932, 2887, 1635, and 1384 cm^{-1} represent the presence of —CH_2, —CH_3, —CO groups and C—O stretching, respectively.[10] After 45 days of exposure, the presence of carbonyl group was evident in spectra [Figure 2(d-2,f-2)]; the band that represents this structural change appears at 1712 cm^{-1} in both the compatibilized and uncompatibilized films; these films had CI values of 3 and 1.6, respectively (Figure 3). The area of the band at 1712 cm^{-1} increased significantly faster with respect to weathering time for PE/chitosan films, compared with PE films (Figure 3); as displayed by the value of CI, an increase in carbonyl groups produced due to photodegradation of the samples is evident; the values of CI for uncompatibilized and compatibilized films, at 180 days, are 37.5 and 52, respectively (Figure 3).

The PE/chitosan films were promptly oxidized, as shown by the rapid increase in carbonyl levels. Clearly, typical photo-

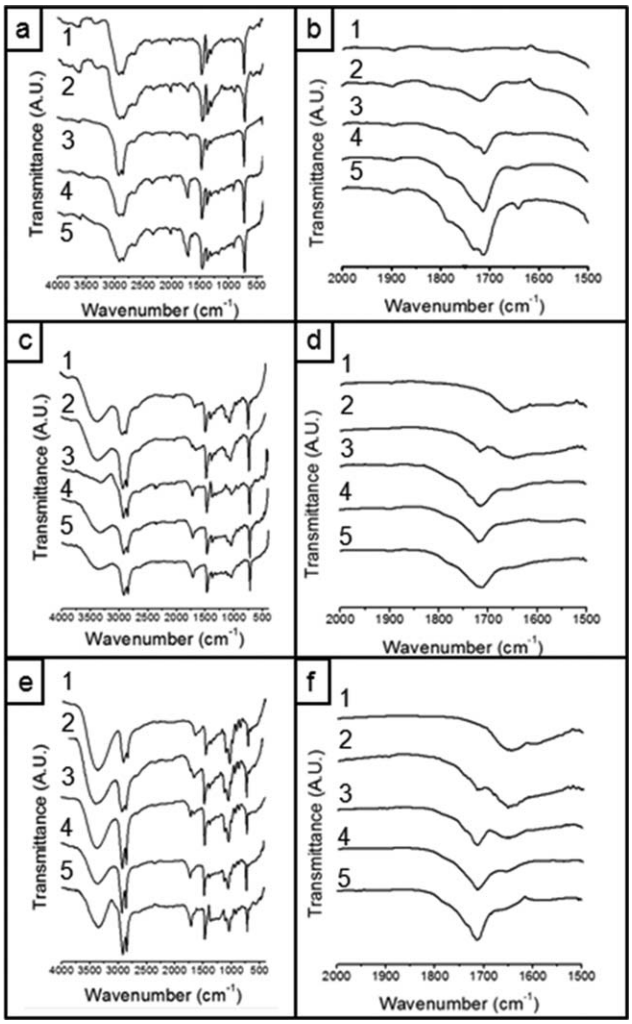

Figure 2. FTIR spectra of (a, b) A film, (c, d) B film, and (e, f) C film, recorded at 0, 45, 90, 135, and 180 natural weathering days (1–5, respectively).

oxidation products of PE, namely carbonyl group at 1712 cm^{-1}, also appeared during the photo-oxidation of the chitosan containing samples, regardless of the presence or absence of PEgMA. Although the compatibilizer appears to not play a determinant role in the overall photo-oxidation mechanism, it does have an accelerating effect on the rate of oxidation of chitosan-containing polymers. The positive effect of PEgMA on the rate of photo-oxidation of the films, evidenced by CI values, could be attributed to the photo-oxidative instability of maleic anhydride,[18] and the possible interactions between the anhydride group and the chitosan moieties.[17] In particular, the worse interfacial adhesion of the uncompatibilized films compared with the PEgMA containing films could play a role in slowing down the propagation of the degradation toward the PE phase.

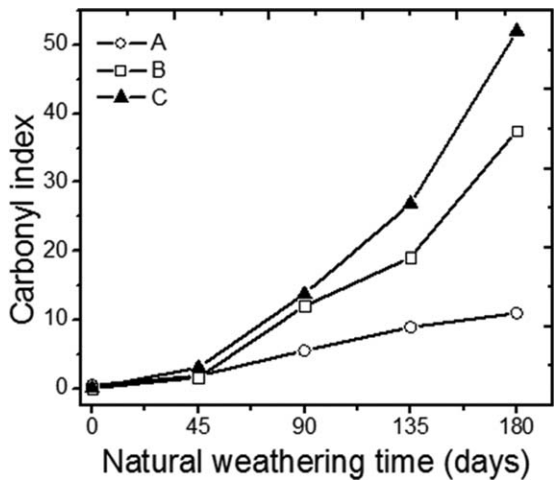

Figure 3. Carbonyl index of films with respect to natural weathering time.

Dehydration and depolymerization are generally considered as two main processes in the polysaccharides' degradation mechanism.[13] With the addition of chitosan, the transmittance of carbonyl groups undergoes similar alterations with increasing weathering time as the observed in film A [Figure 2(d3–5,f3–5)], with the difference that this happens more rapidly. The presence of chitosan favors the degradation of PE; this could be explained considering that chitosan is susceptible to hydrolysis; hydrolysis lowers the molecular weight and increases the amount of aldehyde groups (—CHO) in the open-chain form of chitosan, and these aldehyde groups produce carboxyl groups (—COOH) through photo-oxidation.[29] Various authors report that the presence of oxidation products is a powerful initiator for the degradation of PE.[32]

Mechanical Characterization

Figure 4 shows the dimensionless residual Young's modulus (YM), tensile strength (TS), and elongation at break (EB) reported, as a function of the weathering time. The residual properties were calculated by dividing the values of YM, TS, and EB at different weathering periods of time by the values of the unexposed material. The properties at break, EB in particular, were used to follow the degradation behavior, because of their sensitivity to the structural and morphological variations of the materials occurring during the photo-oxidation.[30]

The mechanical properties of the films changed as exposure time increased (Figure 4). For PE films, YM and TS were not affected during 180 days of natural weathering, showing the typical photodegradation resistant behavior for polyolefins.[1] On the other hand, EB diminished significantly, losing ~50% every 45 days, retaining only 10% of the original elongation when the experiment was completed.

YM for PE/chitosan films [Figure 4(a)] showed an increase of 10% for compatibilized films and 45% for uncompatibilized films and reached a maximum at 45 days. This increase may be explained by crosslinking after the chain scission reactions which could increase film stiffness.[11] YM values significantly decreased at 135 and 180 days, apparently, after 90 days of weathering, the photodegradation process of chitosan starts, showing an improvement in the degradation of the blend films compared with PE; there appears to be no significant difference in YM values between compatibilized and uncompatibilized films.

The PE/chitosan films also experienced a progressive decay in TS [Figure 4(b)] with an 80–90% overall reduction on day 180. The addition of chitosan to PE dramatically affects the natural weathering behavior of the blends; moreover, at 135 days of outdoor exposure, the retention in TS is less than 50%,

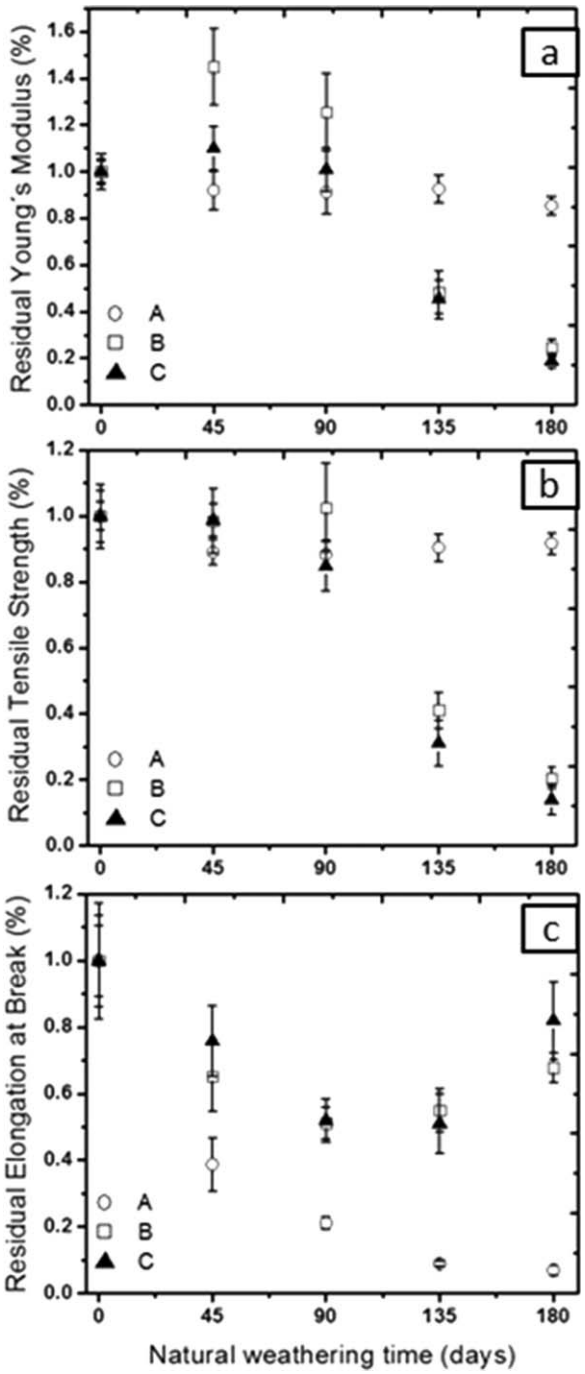

Figure 4. Residual (a) Young's modulus, (b) tensile strength, and (c) elongation at break of (A), (B), (C) films versus natural weathering time; error bars denote standard errors of the means.

therefore, the service life of the material is exceeded[33]; the decay of TS with respect to weathering time is mildly faster in compatibilized films. At 45 and 90 days, the PE/chitosan films became brittle, exhibiting 25–30% reduction in their EB values; this is the expected behavior for synthetic polymers.[24] By 135 days, the samples showed an increase in their elongation, probably because of the advanced state of degradation and an increment in ambient humidity. The compatibilized films showed greater EB values than the uncompatibilized films, indicating a better interaction in the PE/chitosan interface, after natural weathering conditions.

The overall decay in the mechanical properties of PE and PE/chitosan films during weathering may be associated with photochemical alterations leading to a reduction in molecular weight produced by chain scission and crosslinking, which are promoted in turn by photodegradation. Therefore, the addition of chitosan to the PE matrix results in an improvement in the degradation behavior of the film; this is evidenced by the greater decrease in YM and TS after 135 days of natural weathering; PEgMA appears to have a mild accelerating effect in the degradation rate of the PE/chitosan films.

Morphological Characterization

As weathering time increased, the surface morphology of PE changed slightly, losing its characteristic gloss after 45 days; no cracks or fractures were observed neither by visual inspection [Figure 5(a)] nor using the stereo-microscope at any weathering time (Fig. 6, row 1).

The surface of the PE/chitosan films containing PEgMA as a compatibilizer was smoother, and the chitosan particles were less noticeable and better dispersed in the polymer matrix. Chitosan-containing films, both compatibilized and uncompatibilized, changed dramatically in color and appearance. Initially, the surface of the films was smooth and almost translucent, whereas at 45 days, a yellowish coloration was evident; this yellow-brown color intensified and peaked at 90 days [Figure 5(b,c)]. After 135 days of weathering, the coloration diminished and the films' surface became opaque, irregular, and rough; degradation became

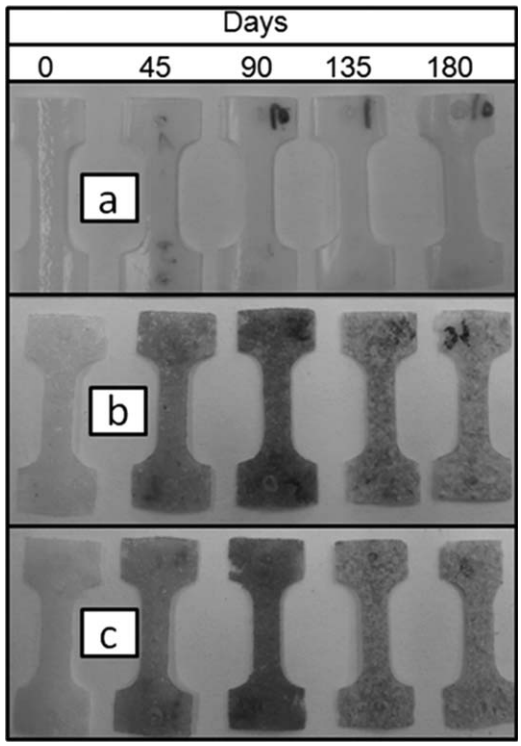

Figure 5. Images of a typical specimen of (a) A, (b) B, and (c) C films after different natural weathering periods of time.

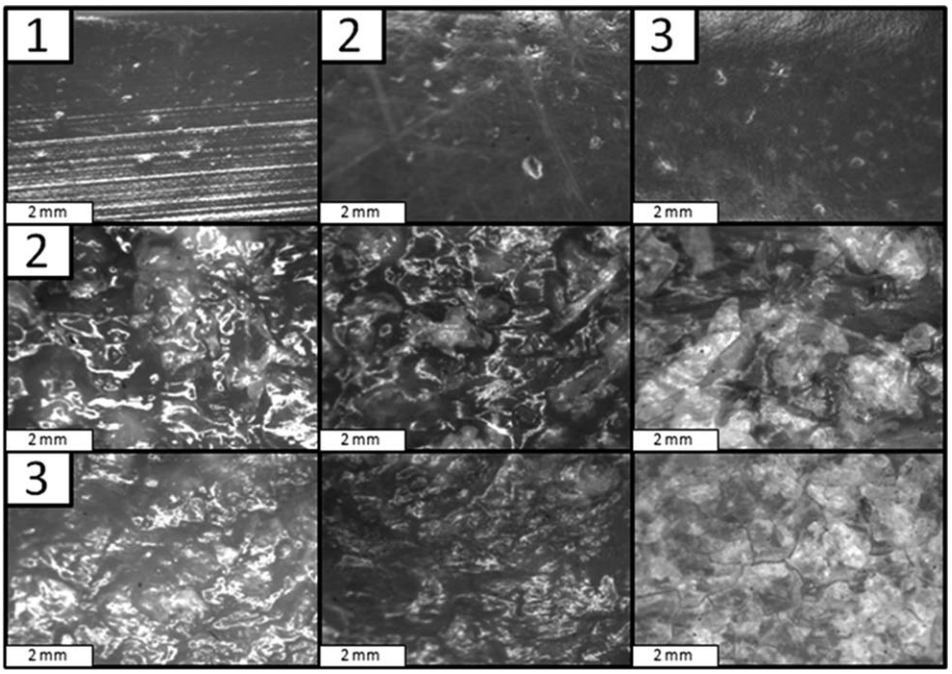

Figure 6. Stereo microscope images of the surface of (row 1) A, (row 2) B, and (row 3) C films, after (column 1) 0, (column 2) 90, and (column 3) 180 natural weathering days.

much more evident in the films and a network of microfractures and holes in different patterns were clearly observed over the surface (Figure 6, rows 2, 3).

Figure 7 shows the SEM micrographs of the films' surface. Before weathering, the surface of film A was smooth and homogeneous [Figure 7(a)], at 90 days of weathering, randomly distributed spots and lines appeared among large unaltered areas [Figure 6(b)], and at 180 days, the surface was covered by microfractures [Figure 7(c)].

The addition of chitosan to the polymeric matrix significantly altered the film surface morphology. The chitosan particles were completely embedded in PE and could not be observed [Figure 7(D,G)]; at 90 days of weathering, small spots appeared and the chitosan particles were much more evident

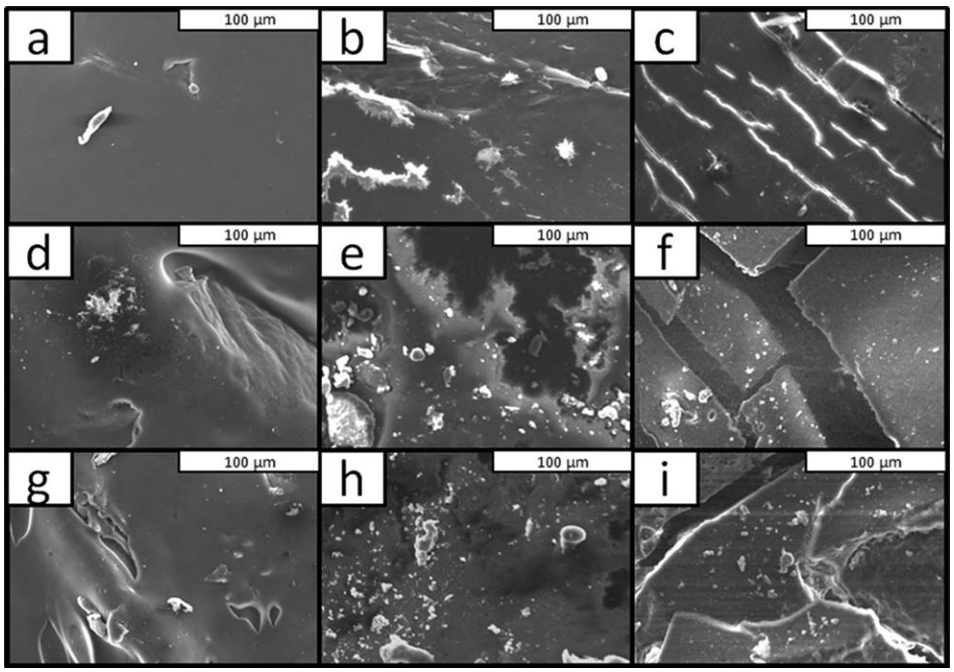

Figure 7. SEM micrographs of the surface of (a–c) A, (d–f) B, and (g–i) C films, after (column a) 0, (column b) 90, and (column c) 180 natural weathering days.

[Figure 7(e,h)], at 180 days of weathering, the surface was clearly degraded. Holes and fractures in different patterns were clearly observed in the surface of the compatibilized and uncompatibilized films [Figure 7(f,i)].

The surface of the PEgMA-containing films appeared to be more homogeneous than the other films; the chitosan particles remained embedded in PE at any weathering time and the cracks and fractures present at the end of the test were smaller and distributed in an apparently more uniform manner, compared with the uncompatibilized films.

Film A was the only polymer without visible cracks or fragmentation after 180 days of exposure; these results are in accordance with the measured mechanical properties of film A, which also decayed more slowly compared with the films that contained chitosan. The addition of chitosan to PE accelerated significantly the degradation behavior of the films.

CONCLUSIONS

The degradation behavior of compatibilized and uncompatibilized PE/chitosan extruded blends was studied, and the structural and physicomechanical properties were monitored. Photodegradation and fluctuations in temperature and humidity led to deterioration of the materials. An accurate characterization, before and after natural weathering, revealed a significant effect of chitosan on the morphology of the films.

PE films containing 15 wt % of chitosan were severely degraded in less than 6 months of exposure to natural weathering. The oxidative degradation produces a significant increase in the content of carbonyl groups. The exposure also led to the formation of microfractures and polymer embrittlement with the concomitant variation of the mechanical properties. The extremely high temperatures and irradiance recorded in the weathering location during the test period, and the use of PEgMA as a compatibilizer enhanced the degradation rate of the films.

The PE/chitosan degradation behavior data reported here will be important in further research on potential uses of chitosan as an environmentally friendly solution to the problem of plastic packaging disposal.

ACKNOWLEDGMENTS

J.M. Quiroz-Castillo acknowledges CONACYT (Consejo Nacional de Ciencia y Tecnología, México) for the financial support provided during this study.

REFERENCES

1. Ojeda, T.; Freitas, A.; Birck, K.; Dalmolin, E.; Jacques, R. *Polym. Degrad. Stab.* **2011**, *96*, 703.
2. Karaduman, A. *J. Energy Sources* **2002**, *24*, 667.
3. Luckachan, G.; Pillai, C. *J. Polym. Environ.* **2011**, *19*, 637.
4. Singh, B.; Sharma, N. *Polym. Degrad. Stab.* **2008**, *93*, 561.
5. Corrales, T.; Catalina, F.; Peinado, C.; Allen, N.; Fontan, E. *J. Photochem. Photobiol.* **2002**, *147*, 213.
6. Guadagno, L.; Naddeo, C.; Vittoria, V.; Camino, G.; Cagnani, C. *Polym. Degrad. Stab.* **2001**, *72*, 175.
7. Gugumus, F. *Polym. Degrad. Stab.* **1993**, *39*, 117.
8. Andrady, A. *Adv. Polym. Sci.* **1997**, *128*, 49.
9. Sionkowska, A.; Planecka, A.; Kozlowska, J.; Skopinska-Wisniewska, J.; Los, P. *Carbohydr. Polym.* **2011**, *84*, 900.
10. Andrady, A. L.; Hamid, S. H.; Hu, X.; Torikai, A. *J. Photochem. Photobiol. B* **1998**, *46*, 96.
11. Kong, X.; Qi, H.; Curtis, J. M. *J. Appl. Polym. Sci.* **2014**, *131*, 40579.
12. Liu, X.; Yu, L.; Xie, F.; Petinakis, E.; Sangwan, P.; Shen, S.; Dean, K.; Ammala, A.; Wong-Holmes, S. *J. Appl. Polym. Sci.* **2013**, *130*, 2282.
13. Freile-Pelegrín, Y.; Madera-Santana, T.; Robledo, D.; Veleva, L.; Quintana, P.; Azamar, J. A. *Polym. Degrad. Stab.* **2007**, *92*, 244.
14. Raghavan, D.; Emekalam, A. *Polym. Degrad. Stab.* **2001**, *72*, 509.
15. Correlo, V. M.; Boesel, L. F.; Bhattacharya, M.; Mano, J. F.; Neves, N. M.; Reis, R. L. *Mater. Sci. Eng. A* **2005**, *403*, 57.
16. Omura, M.; Tsukegi, T.; Shirai, Y.; Nishida, H.; Endo, T. *Ind. Eng. Chem. Res.* **2006**, *45*, 2949.
17. Ermolovich, O. A.; Makarevich, A. V. *Russ. J. Appl. Chem.* **2006**, *9*, 1526.
18. Dintcheva, N. T.; Al-Malaika, S.; La Mantia, F. P. *Polym. Degrad. Stab.* **2009**, *94*, 1571.
19. Del Castillo-Castro, T.; Castillo-Ortega, M. M.; Herrera-Franco, P. J.; Rodríguez-Félix, D. E. *J. Appl. Polym. Sci.* **2011**, *119*, 2895.
20. Zelenetskii, A. N.; Volkov, V. P.; Artemeva, N. Y.; Sizova, M. D.; Nikolskaya, V. P.; Egorova, N. A. *Cent. Eur. J. Chem.* **2003**, *3*, 277.
21. Akopova, T. A.; Vladimirov, L. V.; Zhorin, V. A.; Zelenetskii, A. N. *Polym. Sci. Ser. B* **2009**, *51*, 3.
22. Harish Prashanth, K. V.; Tharanathan, R. N. *Trends Food Sci. Technol.* **2007**, *18*, 117.
23. Pillai, C. K. S.; Paul, W.; Sharma, C. P. *Prog. Polym. Sci.* **2009**, *34*, 641.
24. Sindhu, M.; Abraham, T. E. *Food Hydrocolloids* **2008**, *22*, 826.
25. Makarios-Laham, I.; Lee, T. C. *J. Environ. Polym. Degrad.* **1995**, *3*, 31.
26. Rutiaga, M. O.; Galan, L. J.; Morales, L. H.; Gordon, S. H.; Imam, S. H.; Orts, W. J.; Glenn, M.; Nin, K. A. *J. Polym. Environ.* **2005**, *13*, 185.
27. Quiroz-Castillo, J. M.; Rodriguez-Felix, D. E.; Grijalva-Monteverde, H.; Del Castillo-Castro, T.; Plascencia-Jatomea, M.; Rodriguez-Felix, F.; Herrera-Franco, P. J. *Carbohydr. Polym.* **2014**, *101*, 1094.
28. Al-Aruri, S. D. *Solar Energy* **1990**, *45*, 61.
29. Roy, P. K.; Surekha, P.; Rajagopal, C.; Chatterjee, S. N.; Choudhary, V. *Polym. Degrad. Stab.* **2007**, *92*, 1151.
30. Dintcheva, N. T.; Filippone, G.; La Mantia, F. P.; Acierno, D. *Polym. Degrad. Stab.* **2010**, *95*, 527.
31. Day, M.; Shaw, K.; Cooney, D.; Watts, J.; Harrigan, B. *J. Environ. Polym. Degrad.* **1997**, *5*, 137.
32. Sun, C.; Qu, R.; Chen, H.; Ji, C.; Wang, C.; Sun, Y.; Wang, B. *Carbohydr. Res.* **2008**, *343*, 2595.
33. Al-Salem, S. M. *Mater. Des.* **2009**, *30*, 1729.